International Journal of Mass Spectrometry 281 (2009) 41–51

Contents lists available at ScienceDirect

International Journal of Mass Spectrometry

journal homepage: www.elsevier.com/locate/ijms

Analyte distributions in MALDI samples using MALDI imaging mass spectrometry

Hui Qiao, Gamini Piyadasa [1], Victor Spicer, Werner Ens *

Department of Physics and Astronomy, University of Manitoba, Winnipeg, Canada R3T 2N2

ARTICLE INFO

Article history:
Received 10 October 2008
Received in revised form
27 November 2008
Accepted 27 November 2008
Available online 6 December 2008

Keywords:
MALDI imaging
Analyte incorporation
MALDI crystals
Orthogonal TOF
Analyte segregation

ABSTRACT

The analyte distributions in matrix-assisted laser desorption/ionization (MALDI) samples have been studied using MALDI imaging at better than 10 μm spatial resolution in an orthogonal-injection TOF instrument. The technique is demonstrated by mapping the analyte distribution in typical preparations of MALDI samples using the common matrices 2,5-dihydroxybenzonic acid (2,5-DHB), sinapinic acid and 4-hydroxy-α-cyanocinnamic acid (α-HCCA). These results show evidence of exclusion of impurities, and confirm that smaller matrix crystal size gives better reproducibility from spot to spot. Large single crystals of DHB and sinapinic acid were grown to examine the incorporation of analytes within the crystals. Purified protein analytes were found to be homogenously incorporated in both types of crystal, with no evidence for preferred crystal faces. The distributions of analytes in simple mixtures in single crystals of DHB were also examined. Segregation of some species was observed and appeared to correlate with analyte hydrophobicity, and to a lesser extent analyte mass or mobility. Similar segregation phenomena were observed with fluorescence microscopy of analytes labeled with fluorescent dyes in large 2,5-DHB single crystals, and in smaller crystals grown by fast evaporation. The above investigations may shed some light on optimizing sample preparation with different matrices.

1. Introduction

Since the introduction of matrix-assisted laser desorption/ionization (MALDI) mass spectrometry in 1988 [1,2], it has become a powerful tool in biomolecular analysis [3]. Different matrices [4–6] and sample preparation procedures [1,7–9] have been proposed, with significant differences in mass spectral sensitivity, resolution and reproducibility. It is generally accepted that the matrix absorbs the laser energy and undergoes a phase change, producing isolated intact gas-phase ions of the imbedded analyte molecules. However, the mechanisms behind the interaction of matrix and analyte molecules inside the MALDI matrix crystal before ablation are still not fully understood.

The incorporation of analytes into MALDI matrices has been investigated by several laboratories [10–16]. Strupat et al. showed that proteins are incorporated into slowly grown single crystals of 2,5-dihydroxybenzonic acid (2,5-DHB) and succinic acid, by analyzing redissolved crystals [5,10]. Using X-ray crystallography, they also showed that the crystal structure is unperturbed by the presence of the protein doping [10], suggesting a solid solution [3]. The incorporation of dye-labeled proteins in 2,5-DHB was later shown to be homogenous, using confocal laser scanning microscopy, which also showed that labeled proteins are excluded from crystals of 2,6-DHB [11].

Beavis and Bridson studied the interaction of sinapinic acid with dye-labeled proteins and observed an incorporation pattern resembling an hourglass shape [12]. They suggested that proteins are preferentially or exclusively incorporated into the more hydrophobic face of a single sinapinic acid crystal. However, Mitchell et al. have questioned these conclusions: they observed the identical hourglass-shaped zone with neat dye incorporation at the hydrophobic surface [13]. Moreover, Strupat et al. argue from crystallographic data that there are no major hydrophobic domains in succinic acid and DHB crystals, so incorporation of proteins in these crystals must be based on non-hydrophobic interactions.

Dai et al. used confocal laser scanning microscopy to investigate the incorporation of analytes in 2,5-DHB and sinapinic acid matrix crystals formed by fast and slow evaporation methods [14]. The results show uniform protein incorporation in the slowly grown crystals, but non-uniform distribution of protein analyte in dried-droplet preparations. Their results also show evidence of analyte segregation in simple mixtures in crystals formed by fast evaporation.

Most investigations of analyte incorporation in matrices to date have involved the use of an intermediate label: dye-labeled proteins (horse skeletal myoglobin) [12] and pH indicator dyes [15],

* Corresponding author. Tel.: +1 204 474 6178; fax: +1 204 474 7622.
E-mail address: w_ens@umanitoba.ca (W. Ens).
[1] Present address: Department of Physics, University of Colombo, Colombo, Sri Lanka.

1387-3806/$ – see front matter © 2008 Elsevier B.V. All rights reserved.
doi:10.1016/j.ijms.2008.11.015

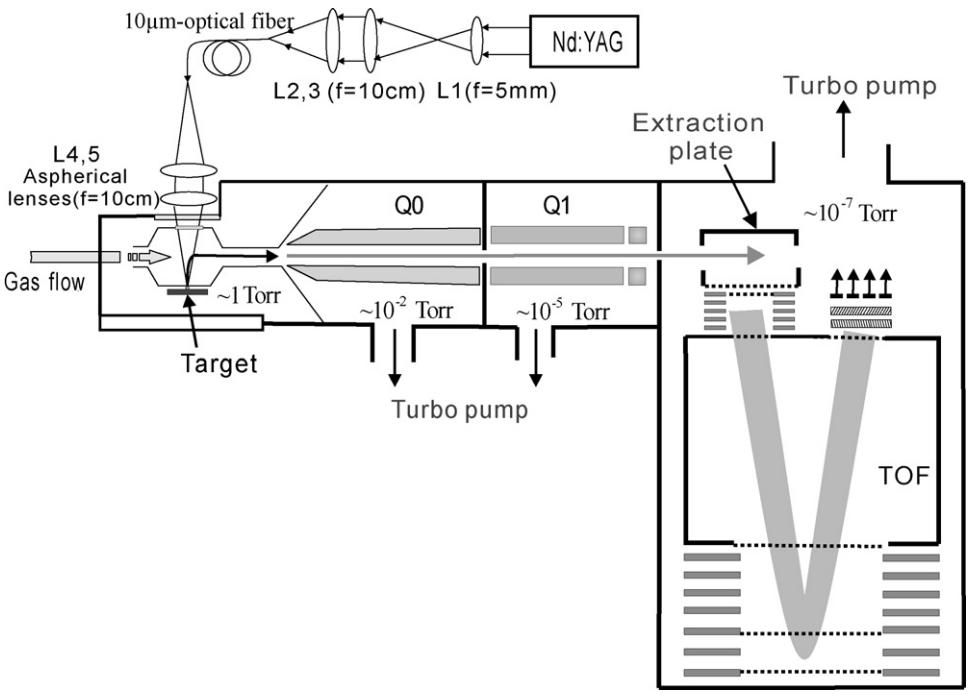

Fig. 1. Schematic diagram of the orthogonal MALDI imaging mass spectrometer.

fluorescence-labeled proteins (fluorescein isothiocyanate (FITC) [14], Texas Red-labeled avidin [11]) and Au-labeled proteins [16]. These labels may affect the properties of analytes, or the presence of unbound labels may mask the properties of the analytes [13]. Moreover, the use of labels introduces additional complexity to the experiment. For example, when using fluorescent materials in confocal laser scanning microscopy, the proper way of labeling proteins, removing the excess dyes, the pH dependence, the variations of the fluorescence intensity for different proteins, and the influence of the refractive index mismatches and the birefringence of the crystals all need to be carefully considered.

MALDI imaging mass spectrometry [17,18] avoids the problems described above. The technique was developed to analyze thin-layer chromatograms [17], and for the study of biological tissue [19,20], but clearly offers the most direct way to study the distribution of analyte in MALDI samples. However, most MALDI imaging systems have rather modest spatial resolution in the range of 100 μm. Garden and Sweedler improved this to about 25 μm to study the heterogeneity of different types of MALDI sample preparation [21], but this was not sufficient to study the incorporation of analyte in individual crystals. We have recently constructed a MALDI imaging instrument with spatial resolution in the range of 10 μm [22], and have reported preliminary results of analyte incorporation in large MALDI crystals, demonstrating homogenous incorporation of pure analytes, but segregation of the components of some mixtures [23]. Bouschen and Spengler have reported even better spatial resolution of about 1 μm, and have shown segregation of analytes in small DHB crystals in dried-droplet preparations [24].

Here we report more detailed investigations of analyte distributions in MALDI matrices using a custom MALDI imaging mass spectrometer with better than10 μm spatial resolution. We first map the analyte distribution on typical preparations of MALDI samples using the common matrices. Then large single crystals of DHB and sinapinic acid were grown to examine the incorporation of analytes within the crystals. For comparison, some fluorescence microscopy is also used to examine the analyte distribution with dye-labeled proteins in 2,5-DHB crystals.

2. Experimental

2.1. Mass spectrometer

The experiments were performed on a modified QStar instrument [25], supplied by MDS Sciex (Concord, ON, Canada), shown schematically in Fig. 1. A novel MALDI source was constructed in which the ions are ejected perpendicular to the axis of the collisional cooling ion guide. This allows normal incidence for the desorbing laser, and closer placement of the final focusing optic, both of which facilitate improved spatial resolution.

For these experiments, the beam from a Nd:YAG laser (JDS Uniphase, model S355B-100Q, Manteca, CA) operated at 1 kHz repetition rate was coupled through a 3-lens optical system into 2-m long fiber optic patch cord, 10 μm in diameter (OZ Optics Ltd., Ottawa, Canada). The fiber had a step-index profile with a numerical aperture ~0.22. Alignment was performed with an attenuated beam by maximizing the transmitted intensity, and then backing the fiber off about 10–20 μm to avoid damaging the end. The fiber output was imaged onto the target with two custom-made 10-cm focal length aspherical lenses (R. Mathews Optical Works, Inc., Poulsbo, WA, USA) arranged in infinite conjugation. This arrangement allowed the laser spot size to closely approximate the fiber diameter (10 μm) [26]. The fluence was kept above the value at which the yield saturates, significantly higher than that typically used in MALDI experiments [26].

The target is mounted on a robotic microstepping 2D-positioner with a relative positioning resolution of 0.5 μm (PI-Physik Instrumente, L.P., Auburn, MA, USA). The image is generated by rastering the target with the laser in a fixed position. Desorbed ions are drawn into the ion guide through a 4 mm diameter cone by a combination of gas flow and an electric field set up by a small, segmented cell. Two rf-only quadrupole ion guides were used, one with segmented

Table 1
List of peptides and proteins used for the study.

Name and amino acid sequence	MW (Da)	(B&B index [27])	Hydrophobicity (GRAVY index [28])
Enkephalin (YAGFLR)	726	−2490 (hydrophobic)	0.368 (hydrophobic)
Substance p (RPKPQQFFGLM)	1,347	−1790 (hydrophobic)	−0.7 (hydrophilic)
Bacitracin [29a] (ICLEIKNDHFI)	1,422	−4000 (hydrophobic)	0.455 (hydrophobic)
Melittin (GIGAVLKVLTTGL PALISWIKRKRQQ)	2,845	−4470 (hydrophobic)	0.273 (hydrophobic)
Horse heart cytochrome C sequence [29b]	12,327	7350 (hydrophilic)	−0.321 (hydrophilic)
Bovine pancreas trypsin inhibitor sequence [29b]	23,460	5780 (hydrophilic)	−0.036 (hydrophilic)
Bovine serum albumin sequence [29b]	66,430	−22,220 (hydrophobic)	−0.433 (hydrophilic)

rods to reduce transit time. The TOF portion was modified to operate with 11 kV acceleration voltage.

2.2. Sample preparation

The matrices, DHB, trans-3,5-dimethoxy-4-hydroxy-cinnamic acid (sinapinic acid, SA) and 4-hydroxy-α-cyanocinnamic acid (α-HCCA), were purchased from Sigma–Aldrich Company (Ontario, Canada) and were used without further purification. The peptide and protein analytes are listed in Table 1. All peptide and protein samples were obtained from Sigma–Aldrich Company (Ontario, Canada), except enkepahlin, which was obtained from American Peptide Company (Sunnyvale, CA, USA). The hydrophobicity of these analytes is calculated according to the B&B index [27] and the GRAVY index [28], which use different hydrophobicity scales of the amino acid residues.

Samples were prepared using the standard dried-droplet [1], thin-layer [7] and crushed crystal preparation methods [8]. In the dried-droplet method, 2,5-DHB was dissolved at a concentration of 100 mg/mL in a mixture of acetonitrile/water (1:1, v/v) and 0.1% trifluoroacetic acid (TFA). Sinapinic acid matrix solution was dissolved at a concentration of 20 mg/mL. α-HCCA matrix was prepared using the same solvent to a saturated solution. All analytes were dissolved in bi-distilled water to a concentration of approximately 20 μM, and mixed with the matrix solution to give a molar ratio of analyte to matrix of $\sim 2 \times 10^{-5}$, as typically used in MALDI [30]. A 1.0 μL aliquot of the mixed solution of matrix and analyte was dropped onto the stainless steel target and air-dried.

For the thin-layer preparation, 2,5-DHB matrix was dissolved in ultrapure acetone at a concentration of 100 mg/mL and a 1.0 μL aliquot of this solution was applied on the target. A thin microcrystalline layer of matrix formed after fast evaporation of solvent. Then 0.5 μL of the mixed matrix–analyte solution (above) was applied onto this thin matrix layer. To prepare crushed crystal samples, the same 2,5-DHB solution as prepared in the dried-droplet method was used. A 1.0 μL aliquot of this matrix solution was first spotted on a target. After it crystallized, it was crushed as described in [8], and then the mixed matrix–analyte solution was applied on top of the crushed matrix layer. In both these methods, the application of the analyte solution redissolved some portion of the existing crystals, so the molar analyte-to-matrix ratio was in the range $(1–2) \times 10^{-5}$.

To grow larger crystals [10], 2,5-DHB and sinapinic acid matrices were prepared at concentrations of 100 mg/mL and 20 mg/mL, respectively, with the same solution as used in the dried-droplet method. Matrix solutions were mixed with analyte solution at a final molar analyte-to-matrix ratio of $\sim 2 \times 10^{-5}$. The mixed solutions were swirled in a vortex mixer and centrifuged. The supernatant solutions were taken and divided into vials. These vials were then warmed up to ∼45 °C in a water bath for 30 min and then allowed to cool to room temperature. The vials were then taken out and put in the refrigerator (4 °C) with the vial lid open for about 2 days in a dark place. Occasionally, single crystals as large as 1 mm × 0.6 mm × 0.4 mm (DHB) and 1 mm × 0.3 mm × 0.2 mm (SA) were obtained. The crystals were washed in the bi-distilled water to remove the mother solution coated on the surface of the crystal. The single crystals could be fixed to the target with a drop of bi-distilled water.

2.3. Constructing the images

MALDI images were constructed using custom software and hardware. The target motion is controlled by a pre-programmed, multi-axis, stepper-motor controller. It is rastered in one dimension at a fixed velocity of about 250 μm/s, followed by a small step (10 μm) corresponding to the laser spot size in the orthogonal direction. Using a repetition rate of 1 kHz, this corresponds to each sample site exposed to 40 laser shots. The start of each new raster line produces a timing pulse that is recorded by the time-to-digital converter in a dedicated channel for later synchronization; the position on the target correlates with elapsed experiment time. The data acquisition system records all the time-of-flight events for an experiment in a memory-spooled file (typically hundreds of megabytes in size). Spools were analyzed off-line to reconstruct mass-dependant images, or mass spectra from selected areas on the target.

2.4. Fluorescence microscopy

Fluorescence microscopy was used to study incorporation of dye-labeled proteins in some MALDI crystals for comparison. The analytes were labeled with two different fluorescent dyes: FITC (Fluorescein isothiocyanate isomer I, Sigma–Aldrich, Ontario, Canada) excited at 488 nm and TRITC (Tetramethylrhodamine isothiocyanate isomer R, Sigma–Aldrich, Ontario, Canada) excited at 561 nm. Simple fluorescent images were obtained with an Olympus BX60 fluorescence microscope (Olympus America Inc. Center Valley, PA, USA), using the 20× magnification lens (NA = 0.5). Confocal scanning laser fluorescence images were obtained with a Zeiss LSM710 microscope (Carl Zeiss Canada Ltd., 45 Valleybrook Dr, Toronto, Canada) with the 10× magnification lens (NA = 0.5).

To label the analyte proteins, the protein solutions were exchanged into borate buffer (pH 8.5, 50 mMol/L) by dialysis for about 2 h using a 500 Da molecular mass cutoff (MMCO) membrane in a beaker containing 2 L of the Borate Buffer, which was placed on a stir plate. The amounts of FITC and TRITC for each labeling reaction were determined depending on the amounts of samples to be labeled. Both dyes were dissolved in DMSO (dimethyl sulfoxide). The concentration of each sample was 10 pmol/μL, and the concentrations of both FITC and TRITC were 10 mg/mL. Dialyzed samples were transferred to a reaction tube and the appropriate amounts of dyes were also transferred to the sample-containing reaction tubes; they were mixed and incubated at room temperature for 1 h. Excess fluorescent dyes were removed by transferring the samples to a new 500 Da MMCO membrane; the samples were dialyzed in PBS (phosphate buffered saline) for about 1 h at room temperature. During dialysis, the samples were stirred and covered with foil to protect the dyes from ambient light. Also the samples labeled with FITC and TRITC were dialyzed separately in different beakers to avoid cross-contamination. After the samples were labeled, they

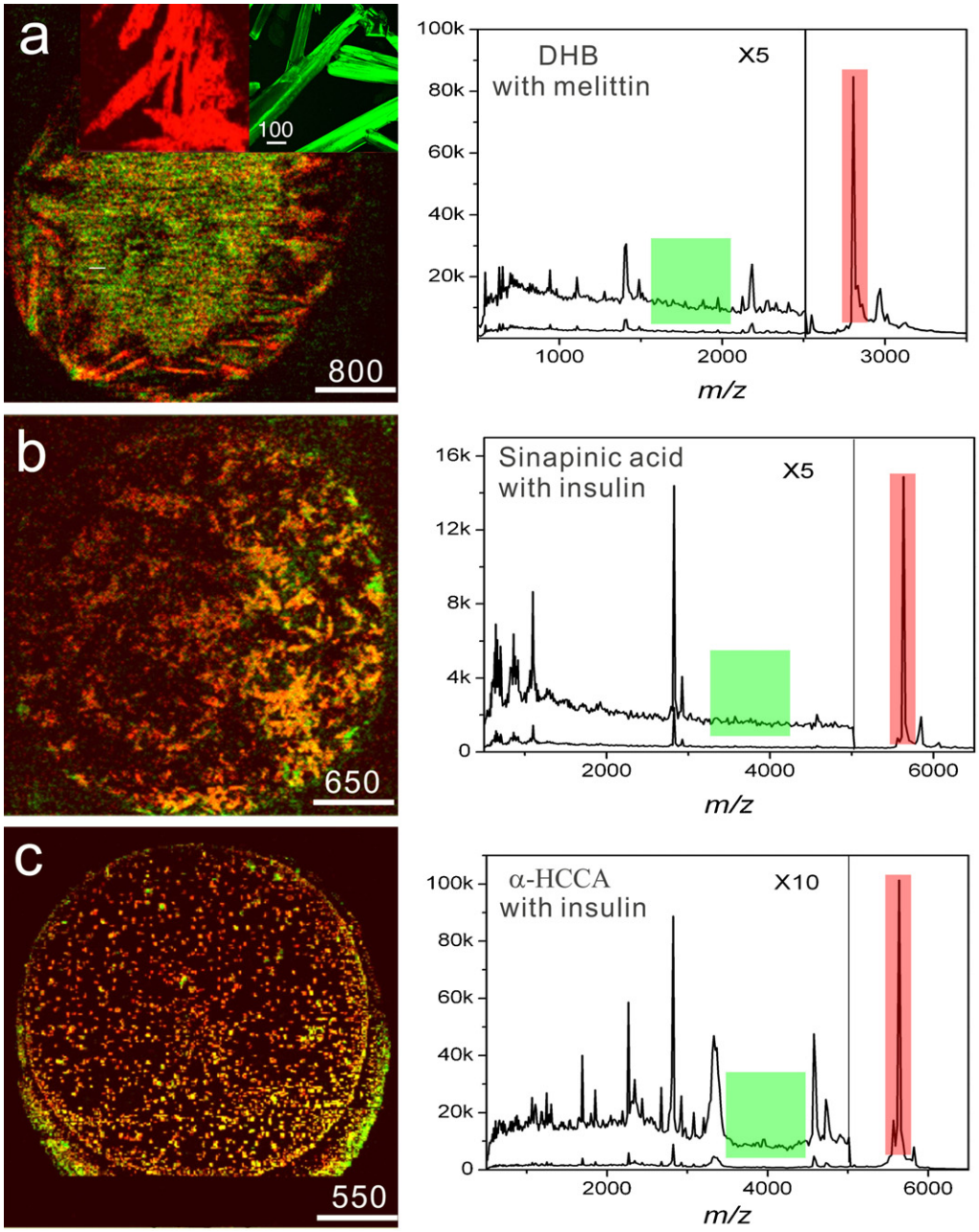

Fig. 2. (a–c) MALDI images of analyte distributions with dried-droplet sample preparation for different matrices and the corresponding integrated mass spectra. Red represents the distribution of analyte molecules and green represents the background chemical noise as indicated in the mass spectra. In panel (a), the inset in red is an expansion of the MALDI image showing crystals near the periphery of the target. The inset in green is a confocal scanning fluorescence image of bacitracin labeled with FITC in a dried-droplet DHB crystal, shown here for comparison. The indicated scales are in μm. (For interpretation of the references to color in this figure legend, the reader is referred to the web version of the article.)

were mixed with DHB matrix solution to grow the DHB single large crystals following the procedure described above.

The acidic matrix solution used strongly quenches the signal from these dyes, particularly from FITC, making relatively long exposures (or high gain) necessary. Images of pure crystals and crystals with only one dye, but illuminated with the frequency for the other dye demonstrated that autofluorescence from the crystal, or other sources of stray light were at least an order of magnitude less intense than the desired fluorescence from the labeled proteins. Even so, in the fluorescence images of the large crystals (where confocal scanning was not used), autofluorescence and internal reflection may be responsible for some diminished contrast in the images.

3. Results and discussion

3.1. Analyte distributions in standard MALDI samples

The empirical distributions of MALDI crystals and analyte signal from different types of sample preparation in MALDI are quite well known, and have been previously mapped at modest resolution by imaging MALDI [21]. In the dried-droplet preparation with DHB, larger crystals tend to form on the periphery of the spot, and the signal tends to be concentrated there in so-called hot spots. For sinapinic acid or α-HCCA, the crystals tend to be smaller and more uniformly distributed over the sample spot. The crushed-crystal and thin film methods of preparation both result in smaller

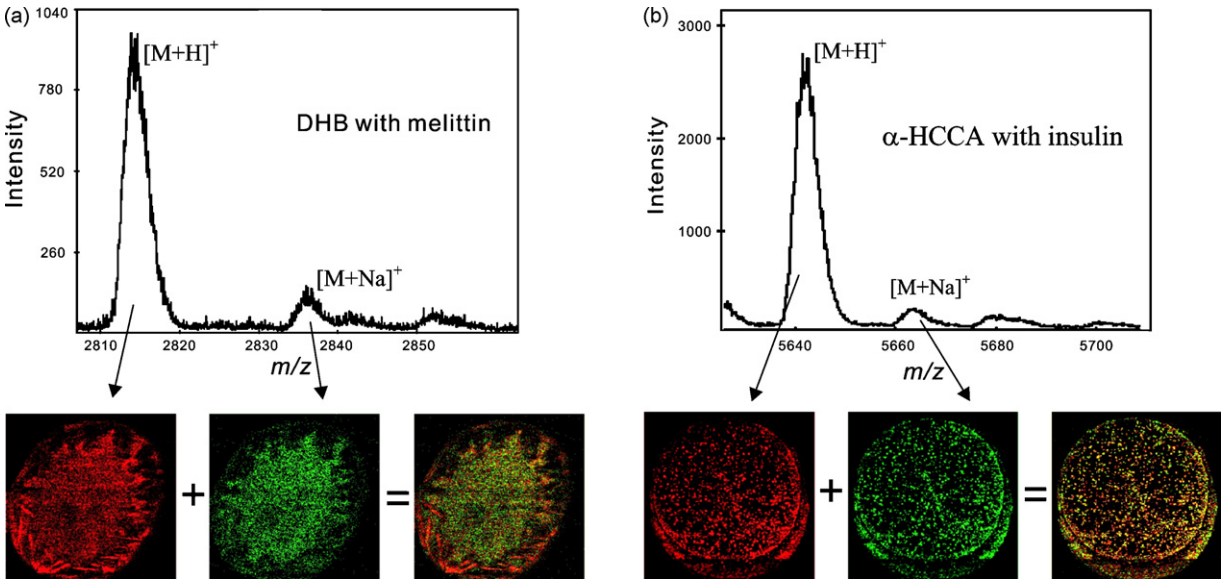

Fig. 3. Distributions of the protonated and sodiated molecular ions in dried-droplet preparations of (a) DHB with melittin (b) α-HCCA with insulin, and the corresponding mass spectra.

average crystal sizes for all the matrices, and consequently a more uniform distribution of signal over the sample. In this section, we examine these common sample preparation techniques at better than 10-μm resolution with different analyte species, mainly to demonstrate the imaging method.

Fig. 2 shows the mass spectra of melittin or insulin from DHB, α-HCCA, and sinapinic acid using the dried-droplet preparation and the corresponding images for the targets. Red represents the distribution of analyte molecules and green represents the background chemical noise as indicated, where no significant peaks are present. As expected, the three matrices give very different sample morphologies corresponding presumably to the way the crystals form during air drying, and is consistent with the description given above.

Fig. 2a shows the results for the DHB sample. The largest crystals are typically about 500 μm in the longest dimension, but less than 100 μm in the other dimensions. It is clear that the analyte molecules (red color) are found mostly around the edge of the sample and located on the macrocrystals of the DHB matrix, consistent with observations of hot spots on the edge of dried-droplet preparations. The results suggest incorporation of the analyte into the crystals. A zoomed image of some DHB macrocrystals is shown in the red inset. Although the analyte distribution over the whole sample (Fig. 2a) is highly non-uniform, the inset suggests that the distribution within the crystals is relatively uniform, consistent with the recent mass spectral images of dried-droplet samples reported by Bouschen and Spengler [24], but in contrast to some observations of sweet spots even within crystals. Our spatial resolution is quite coarse, however, with even the largest faces of the crystals only a few pixels in width, so it is difficult to draw definitive conclusions about uniformity in these small crystals. The other faces are smaller still, and in general not exposed to the laser in dried-droplet samples.

For comparison, we have also examined dried-droplet preparations of bacitracin labeled with FITC in DHB using confocal fluorescence microscopy. The image shown in the green inset in Fig. 2a seems reasonably consistent with the MALDI results, considering the much inferior spatial resolution and dynamic range of the MALDI image. The confocal image does show some non-uniformity, but the distribution is considerably more uniform than observed by Dai et al. using similar methods [14]. This may indicate that the incorporation of analyte in rapidly drying crystals is highly variable, and dependent on particular sample preparation conditions.

Fig. 2b shows relatively small crystals formed from sinapinic acid matrix. The matrix crystals are much smaller than those of the DHB matrix, typically less than 50 μm. The analyte molecules are relatively uniformly distributed around the whole sample, and higher signal reproducibility was obtained from sinapinic matrix than that of the DHB matrix. Fig. 2c shows the α-HCCA sample. The matrix crystal size are much smaller that the above two, typically less than 10 μm. The analyte molecules are more homogenously distributed, giving the best signal reproducibility from spot to spot.

Fig. 2 also shows the distribution of chemical noise for the 3 dried-droplet preparations. In the case of DHB, the chemical noise is distributed more uniformly throughout the sample suggesting their exclusion from the larger crystals, consistent with the high tolerance to impurities observed in MALDI [5,8,24,31]. It is not possible to examine the distribution of sodium in the sample directly in our instrument because of the low mass cutoff of the quadrupole ion guides, but Fig. 3 shows the distribution of the sodium adducts, which is presumably correlated to the sodium distribution. The exclusion of sodium is striking in Fig. 3a, where no signal from the sodium adducts is observed in the large peripheral crystals, consistent with previous electron microprobe analysis and electron microscopy measurements [5] and earlier MALDI imaging results [24]. In Fig. 2b and c, there is some evidence of segregation of the noise signal from the analyte signal in sinapinic acid and α-HCCA targets, with the noise more dominant at the edges of the dried-droplet, in contrast to the DHB sample. Again, the distribution of the sodium adducts in the α-HCCA target shown in Fig. 3b has the same characteristic. The exclusion from the much smaller crystals is much less obvious in this case compared to DHB, but the increased Na signal at the periphery is quite clear.

The segregation of the noise signal to the sample periphery is much more pronounced in the more complex sample shown in Fig. 4, where two crude cell lysates from the K562 human leukemia cell line were mixed with α-HCCA solution and deposited directly on the target without purification. Here the noise is much more pronounced at the edges, and a spectrum taken from the edge shows almost no analyte signal at all.

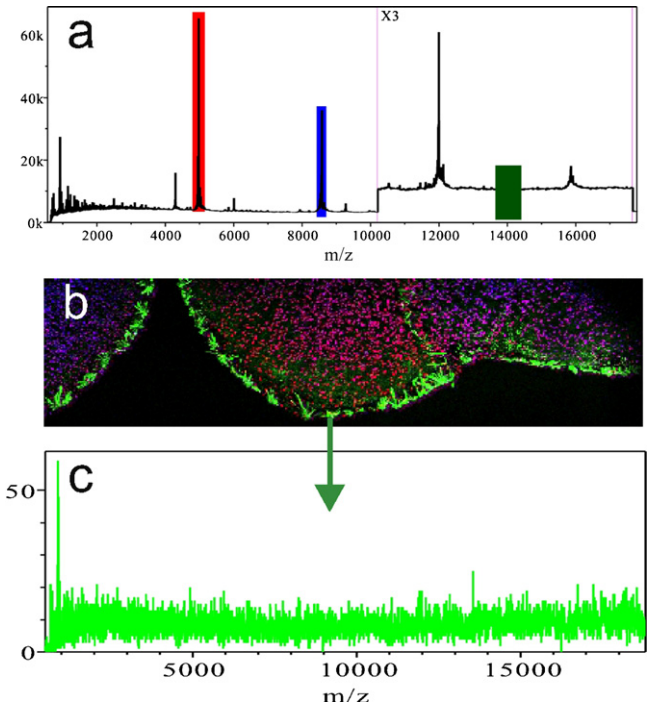

Fig. 4. MALDI images and mass spectra of two cell mixtures prepared with the dried-droplet method without purification. Clear segregation of chemical noise from the analyte signal is observed. (a) Mass spectrum indicating imaged portions by color, (b) corresponding MALDI images and (c) mass spectrum generated from the edge of the sample. (For interpretation of the references to color in this figure legend, the reader is referred to the web version of the article.)

The observed segregation of the noise signal from the analyte signal may indicate that there is a relatively lower affinity of sodium ions with the matrix molecules compared to the protein ions. Therefore the sodium ions may still remain in the solvent solution during the matrix crystallization process instead of incorporating into the matrix crystal as the protein ions. This seems consistent with the distribution of noise signal mostly from the center or between DHB matrix crystals shown in Fig. 2a, and around the edge of the sample shown in Figs. 3b and 4. However, the absence of analyte signal in noisy regions does not necessarily indicate the absence of analyte, since it is well known that salts or other impurities can suppress analyte signal in MALDI, and that signal can often be recovered by sample washing procedures. On the other hand, the absence of noise signal in the regions of strong analyte signal is strong evidence for the absence of impurities.

We also examined the analyte distributions in the thin-layer [7] and crushed crystal [8] sample preparations. For sinapinic acid and α-HCCA, it is well established that the resulting crystals are even smaller, and the signal distribution even more uniform, but the techniques are less commonly used with DHB, which we examine here. As shown in Fig. 5, it is clear that the crystals formed with both methods are smaller and produce a much more homogenous analyte distribution. The crushed crystal method produces the smallest crystals, similar to those of the α-HCCA dried-droplet, while the thin-layer produces intermediate size comparable to the sinapinic acid crystals formed from a dried-droplet.

In summary, the examination of different matrices and preparation methods using MALDI imaging gives a straightforward impression of the analyte distributions. The results show that smaller matrix crystals produced either from different matrices or different sample preparation methods contribute to the uniformity of the analyte distributions across the sample, resulting in better ion signal reproducibility from spot to spot. Experiments like this can be used to provide some guidance about how to choose the suitable matrix and sample preparation methods for a particular application.

3.2. Distributions of purified analytes in single crystals

In the standard MALDI samples investigated above, the crystals are too small to determine detailed analyte distributions within the crystals by MALDI imaging. We have therefore grown single crystals of DHB and sinapinic acid matrices to ~mm dimensions [30] with inclusion of cytochrome C as analyte.

The DHB crystals are mostly parallelepiped up to 1 mm × 0.6 mm × 0.4 mm in size. We examined the largest face (1 0 0), believed to be the face most commonly exposed to the laser during MALDI [10], and the larger cross-section (0 1 0) from the same crystal. The distribution of cytochrome C in this crystal, shown in Fig. 6a and b, indicates homogenous incorporation, which is also manifested by the low variation in the signal intensity from spot to spot when acquiring the mass spectrum. The small variations of the signal on the crystal face appear to be random or statistical in nature, whereas any influence of the crystal growth or crystal properties on incorporation might be expected to exhibit a pattern.

Sinapinic acid forms long crystals along the [1 0 0] axis with a hexagonal cross-section (1 0 $\bar{3}$) [32]; in our case, the crystals are

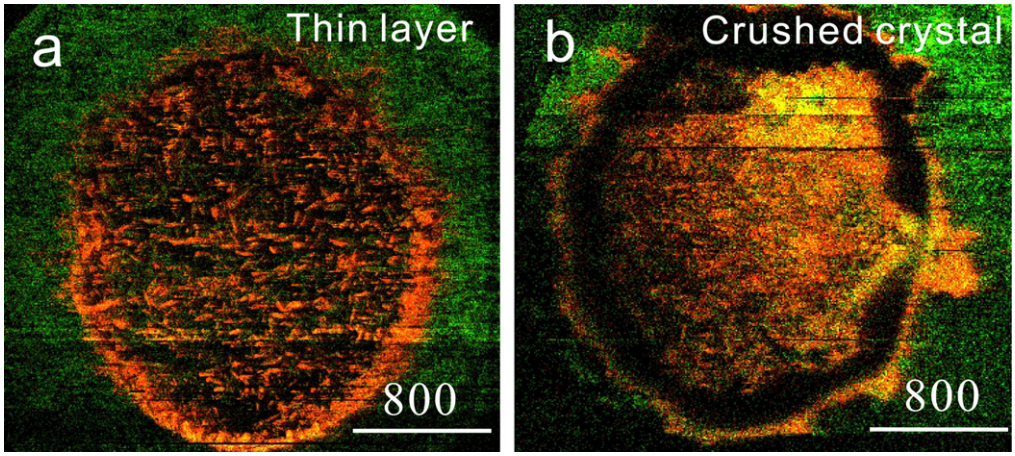

Fig. 5. MALDI images of the distribution of melittin in DHB matrix with thin-layer and crushed crystal sample preparations, using the color scheme of Fig. 2. It is clear that thin-layer and crushed crystal methods give a more homogeneous analyte distribution than that of dried-droplet method. The indicated scale is in μm. (For interpretation of the references to color in this figure legend, the reader is referred to the web version of the article.)

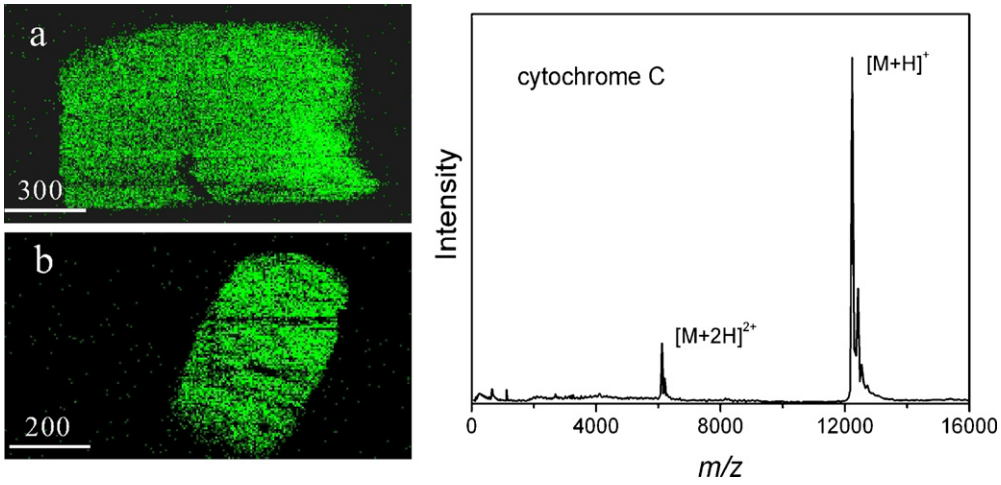

Fig. 6. MALDI images of the distribution of cytochrome C on two faces of a single large DHB matrix crystal, and the corresponding integrated mass spectrum. Analyte molecules are homogeneously distributed on both (a) the largest face (1 0 0) and (b) the larger cross-section (0 1 0). The indicated scale is in μm.

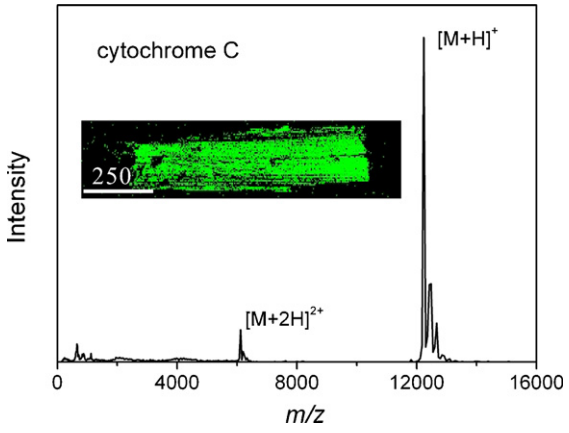

Fig. 7. MALDI image of the distribution of cytochrome C on the largest face (0 1 0) of single crystal of sinapinic acid, and the corresponding integrated mass spectrum. The indicated scale is in μm. Analyte molecules are homogeneously distributed this face. No image was obtained from the cross-section (1 0 $\bar{3}$) of sinapinic acid crystal due to its small dimension.

about 1 mm long with a cross-section of about 0.3 mm along a diagonal. The analyte distribution on the largest face of this crystal (0 1 0), shown in Fig. 7, is again quite uniform, as with the DHB crystal, consistent with the observation of a large sinapinic acid crystal by Dai et al. using confocal fluorescence microscopy [14].

In order to obtain crude depth profiles, all three crystal faces in Figs. 6 and 7, were scanned multiple times. Since each sample site is exposed to 40 laser shots, and the fluence with small spots is high compared to typical MALDI experiments [26], considerable material is removed during each scan. The laser was refocused between scans to optimize the signal, and from the distance the lenses were moved, the ablation depth is estimated to be a few tens of μm.

Fig. 8 shows the results from the first four scans. In each case the intensity decreases, probably as a result of surface modification due to laser irradiation [33], but the distributions remain quite homogenous. This interpretation is consistent with a measurement of a cut crystal, which showed no difference in intensity from an uncut crystal. A small decrease in homogeneity is observed, but again, it appears to be random or statistical, and therefore is also likely to be associated with the lower signal intensity or uneven surface modification, and not inhomogenous incorporation in the crystal.

The depth resolution in these profiles is rather coarse, and may obscure fine structure on the scale of 10 μm or less. However, the lateral images do not show structure on this scale on the faces examined. Moreover, experiments on the hysteresis effect in MALDI by Fournier et al. [32], in which a single spot on a sinapinic acid crystal is examined repeatedly after much smaller irradiation cycles, also show a quite uniform distribution of signal as a function of radiation, and therefore of depth on a considerably finer scale.

To improve the generality of the above observations, we have also examined a much larger protein (BSA at ~66 kDa) in DHB. The results shown in Fig. 9 again show a homogeneous inclusion of the analyte.

These results represent the first direct mass spectrometric measurement of protein distribution within large single crystals of DHB, and within crystals of sinapinic acid (of any size). The results show no evidence for heterogeneous distribution of purified protein analytes neither near the crystal surface nor throughout the crystal. Although we were not able to examine the smaller faces of the crystals, such as the (1 0 $\bar{3}$) face of sinapinic acid, the depth profiles from repeated scans suggest that the distribution in other dimensions is also uniform.

Ejection dynamics are quite different for different MALDI matrices, and this has been correlated to different degrees of analyte incorporation [11,34]. In particular, the initial velocities of analyte ions ejected from 2,5-DHB are considerably higher, and the ions more stable, than from 2,6-DHB, in which evidence suggests only surface adhesion of the analyte [11]. This led to speculation that other matrices with low initial analyte velocities like α-HCCA might also belong to a class of matrices that do not incorporate analytes. However, measurements using pH indicator molecular probes with redissolved crystals give evidence for incorporation of protein analytes in single crystals of α-HCCA [15]. Our results clearly show analyte incorporation in sinapinic acid, and the initial velocities of analyte ions from sinapinic acid are quite close to those ejected from α-HCCA and 2,6-DHB,

The results with DHB are consistent with the more indirect depth profiles and spectrophotometric measurements of redissolved crystals by Strupat et al. [10] and of the confocal microscope images of labeled proteins of Horneffer et al. [11]. In contrast to DHB, the different faces of sinapinic acid have very different hydrophobicity [12], and incorporation of dye-labeled proteins has been reported to occur preferentially (or exclusively) on the hydrophobic face, resulting in an hourglass pattern of proteins on the (0 1 0)

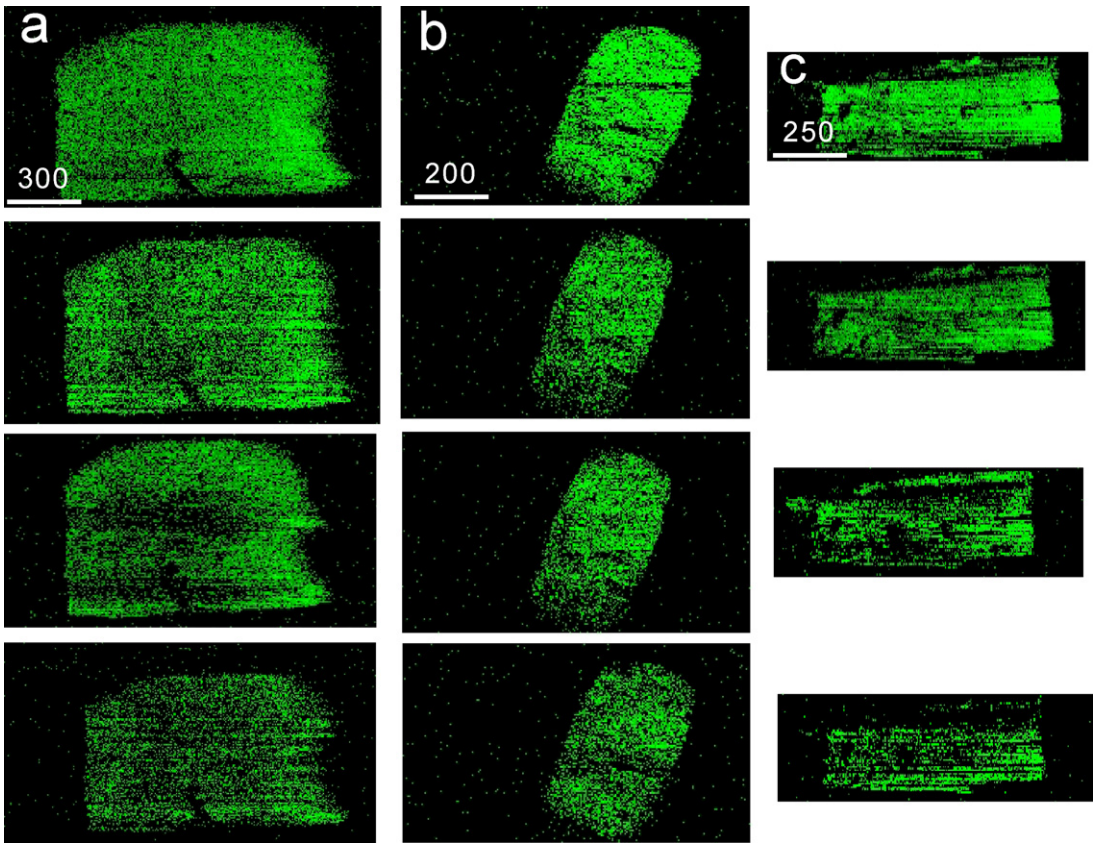

Fig. 8. MALDI images of cytochrome C observed in consecutive scans of (a) the largest face (1 0 0) of DHB single crystals, (b) the larger cross-section face (0 1 0) of DHB single crystals, and (c) the largest face (0 1 0) of sinapinic acid single crystals. The consecutive scans provide a depth profile and demonstrate homogenous incorporation. The variation of intensity is probably a result of surface modification due to laser irradiation (see text).

face. Our results show no evidence of preferential incorporation of pure proteins in sinapinic acid, consistent with the suggestion that the hourglass result may be an artifact from unbound dyes in the solution [13].

3.3. Distribution of multiple analytes in single crystals

Although purified protein analytes appear to be homogenously distributed within large single matrix crystals, we have observed segregation between some analytes when the matrix crystal is doped with a mixture [23]. For example, Fig. 10 shows the analyte distributions of melittin and cytochrome C. It is obvious that they are not homogeneously distributed in the single large crystal, but seem to segregate from each other.

To reduce the possibility of ionization artifacts in MALDI that might produce this kind of a result, we have also used fluorescence microscopy to examine single large crystals doped with the same dye-labeled analytes. Fig. 11 shows simple fluorescence images of (a) melittin labeled with TRITC (red), (b) cytochrome C labeled with FITC (green), and (c) the superposed image of these two analytes. The contrast in this image is probably degraded by autofluorescence and internal reflection, but the pattern clearly shows segregation, consistent with the MALDI images of unlabeled proteins (although different in detail). Better images of small crystals

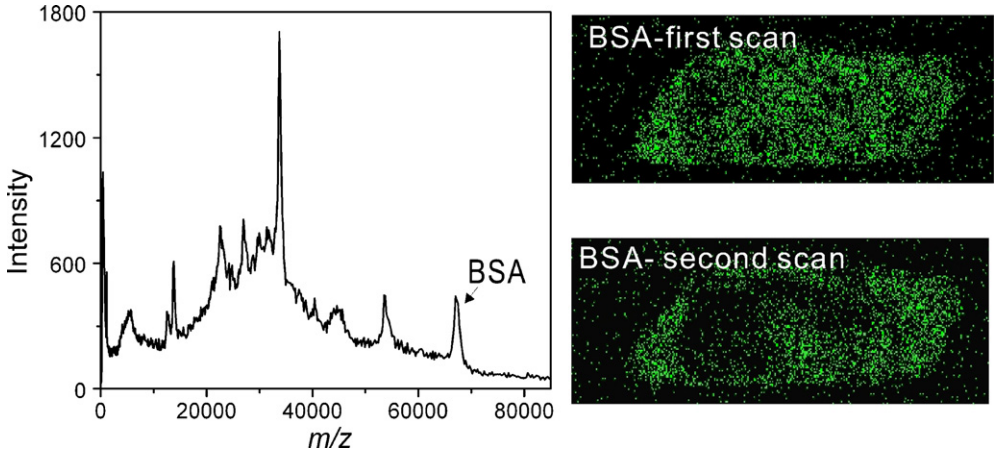

Fig. 9. The analyte distributions of BSA in a DHB single crystal, and the integrated mass spectrum. Two consecutive scans are shown.

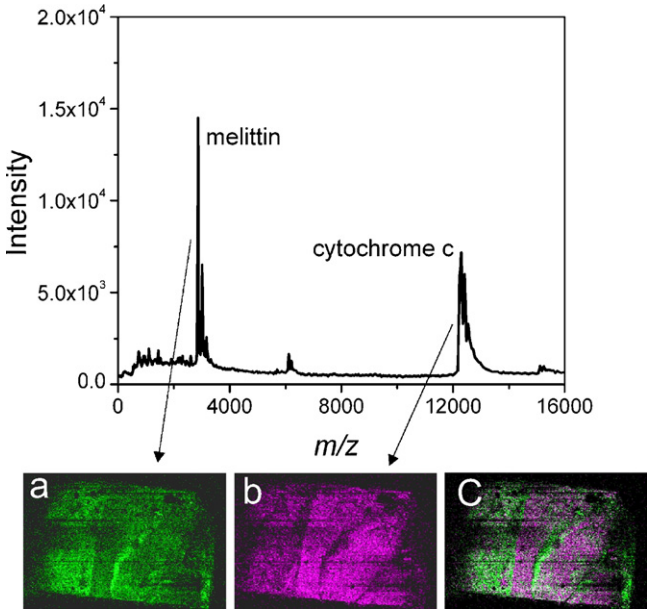

Fig. 10. MALDI images of the analyte distributions of (a) melittin and (b) cytochrome C in a DHB single crystal, and the integrated mass spectrum. The composite image is shown in (c). (To differentiate the colors in the composite image(s), the reader is referred to the web version of the article.)

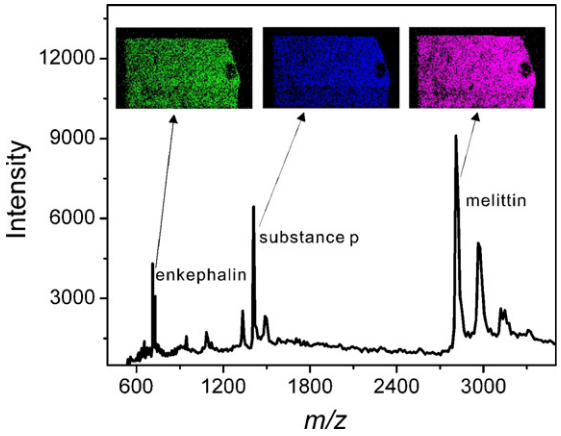

Fig. 12. The analyte distributions of enkephalin, substance p, and melittin in a single DHB crystal. The three analytes have similar hydrophobicity, and no significant analyte segregation is observed.

formed in dried-droplet samples (fast drying), obtained using confocal laser scanning microscopy, are shown in Fig. 11d–f, and also show segregation of the analytes.

Bouschen and Spengler have also observed segregation within crystals formed in the dried-droplet preparation, and they have suggested some dependence of the effect on hydrophobicity (which is closely related to solubility), isoelectric point, analyte mass, and polarity [24]. We have not done systematic measurements to quantify such dependences, but our results do show a strong correlation between segregation and hydrophobicity, particularly as calculated with the B&B index [27], although it is not consistent with the GRAVY index [28] in the case of substance p (see Table 1). The analytes shown in Fig. 10 have very different hydrophobicity with melittin being hydrophobic and cytochrome C hydrophilic. Two three-component mixtures are shown in Figs. 12 and 13. In Fig. 12, all three components are similarly hydrophobic on the B&B index, and no segregation is observed. In Fig. 13, two components are similarly hydrophobic on the B&B index, while the third is strongly hydrophilic and appears segregated from the first two.

The absence of segregation of substance p and melittin in Figs. 12 and 13 is in contrast to the results of Ref. [24] for the same peptides in dried-droplet crystals. The difference here may be related to the much more rapid formation of the crystals in a drying droplet, or the continuous diffusion of an equilibrium solution during the growing of a large crystal.

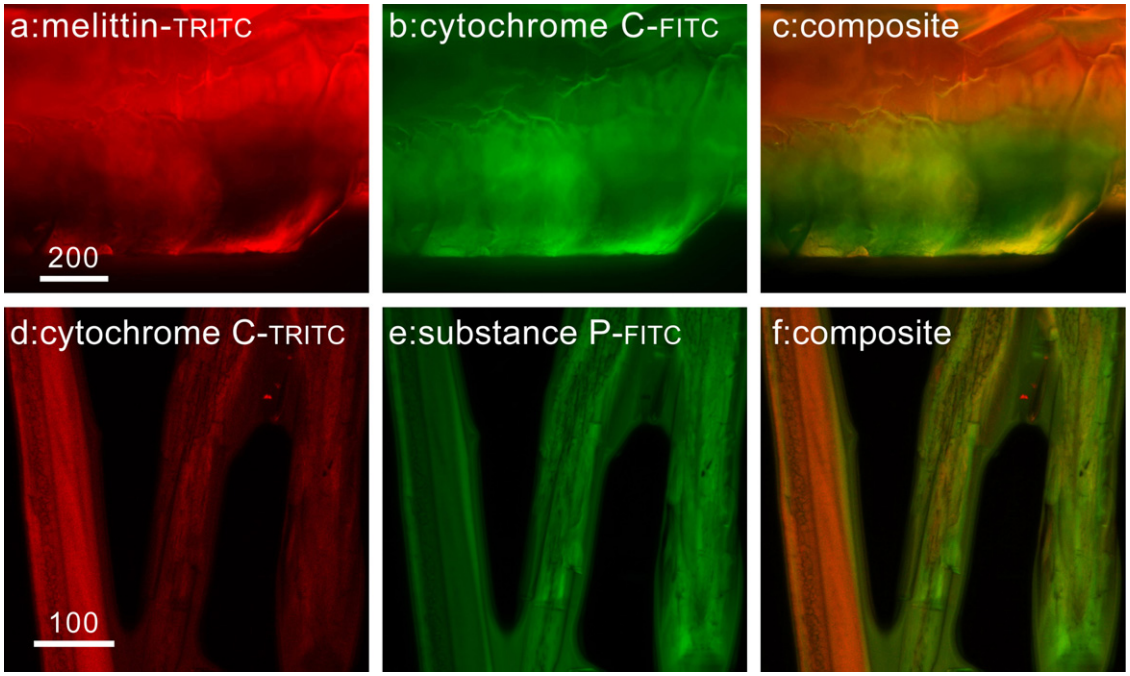

Fig. 11. Flourescence images of (a) melittin-TRITC, and (b) cytochrome C-FITC in a single DHB crystal, with the composite image in (c); and confocal scanning images of (d) cytochrome C-TRITC, and (e) substance P-FITC in crystals of DHB formed in a dried-droplet, with the composite image in (f). Analyte segregation is clearly observed for the slowly grown single crystal using the same analytes as in Fig. 10, and for smaller crystals formed in a dried-droplet. (To differentiate the colors in the composite image(s), the reader is referred to the web version of the article.)

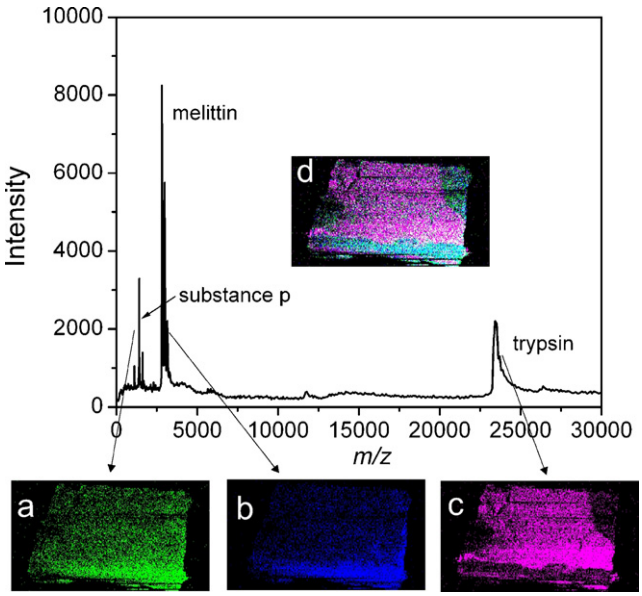

Fig. 13. The analyte distributions of (a) substance p, (b) melittin, and (c) trypsin in a single DHB crystal. The two analytes with similar hydrophobicity (a and b) are segrated from the third (c), which has opposite hydrophobicity. The composite image is shown in (d). (To differentiate the colors in the composite image(s), the reader is referred to the web version of the article.)

The mass difference between the analytes, and the resulting difference in mobility may also play a role in the segregation phenomenon, which is observed in Figs. 10 and 13 where the mass difference (and ratio) are significant. However, this correlation seems less compelling than the hydrophobicity correlation in our results. In Fig. 12, the mass ratio between enkephalin and melittin is close to that of melittin and cytochrome C (Fig. 10), but no obvious segregation is observed. Moreover, in Fig. 14, the mass difference between cytochrome C and trypsin is similar to that between melittin and cytochrome C and again, no segregation is observed.

The mechanism of segregation is not understood, and is probably affected by many parameters including the concentration ratio of analyte solution, the pH value, and the temperature of the matrix solution in addition to the intrinsic properties of the analytes mentioned above. It is clear however that better reproducibility in MALDI (and subsequently better quantification) depends on gaining more control over the segregation and incorporation phenomena. Imaging experiments such as those reported here can play an important role in this type of investigation.

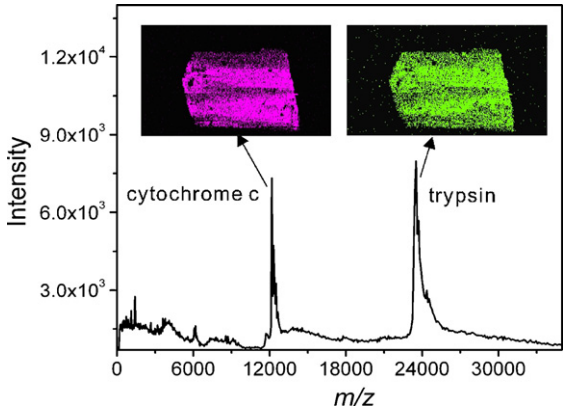

Fig. 14. Analyte distributions of cytochrome C and trypsin in a single DHB crystal. Although the distributions are not perfectly homogenous, no segregation is observed.

4. Conclusions

We have demonstrated the utility of a high resolution MALDI imaging technique for examining analyte distributions in MALDI samples, and in single MALDI crystals. The correlation between smaller crystals and improved reproducibility was verified, and direct evidence for exclusion of impurities in dried-droplet samples was shown.

Purified proteins are incorporated uniformly throughout slowly grown single crystals of DHB and sinapinic acid, with no evidence for preferred crystal faces. In our preparation of dried-droplet samples, the crystals formed by fast evaporation also show reasonably uniform distributions of purified protein analytes in the MALDI images, although higher resolution confocal scanning fluorescence images show some non-uniformity.

Mixtures of protein analytes incorporated in slowly grown DHB crystals show analyte segregation, a phenomenon that appears to be correlated with analyte hydrophobicity.

Acknowledgements

The authors gratefully acknowledge Dr. John Wilkins and Dr. Namita Kanwar for assistance with the fluorescence microscopy and for the K562 leukemia cell lysates, and Dr. Vladimir Collado and Dr. Oleg Krokhin for useful discussions and help with the hydrophobicity estimates. This work was supported by grants from Genome Canada, MDS SCIEX, and from the Natural Sciences and Engineering Research Council of Canada.

References

[1] M. Karas, F. Hillenkamp, Anal. Chem. 60 (1988) 2299.
[2] K. Tanaka, H. Waki, Y. Ido, S. Akita, Y. Yoshida, T. Yoshida, T. Matsuo, Rapid. Commun. Mass Spectrom. 2 (1988) 151.
[3] F. Hillenkamp, M. Karas, R.C. Beavis, B.T. Chait, Anal. Chem. 63 (1991) 1193A.
[4] R.C. Beavis, B.T. Chait, Rapid Commun. Mass Spectrom. 3 (1989) 432.
[5] K. Strupat, M. Karas, F. Hillenkamp, Int. J. Mass Spectrom. Ion Process. 111 (1991) 89.
[6] R.C. Beavis, T. Chaudhary, B.T. Chait, Org. Mass Spectrom. 27 (1992) 156.
[7] O. Vorm, M. Mann, J. Am. Soc. Mass Spectrom. 5 (1994) 955.
[8] F. Xiang, R.C. Beavis, Rapid Commun. Mass Spectrom. 8 (1994) 199.
[9] J. Krause, M. Stoeckli, U.P. Schlunegger, Rapid Commun. Mass Spectrom. 10 (1996) 1927.
[10] K. Strupat, J. Kampmeier, V. Horneffer, Int. J. Mass Spectrom. Ion Process. 169/170 (1997) 43.
[11] V. Horneffer, A. Forsmann, K. Strupat, F. Hillenkamp, U. Kubitscheck, Anal. Chem. 73 (2001) 1016.
[12] R.C. Beavis, J.N. Bridson, J. Phys. D: Appl. Phys. 26 (1993) 442.
[13] C.A. Mitchell, S. Lovell, K. Thomas, P. Savickas, B. Kahr, Angew. Chem. Int. Ed. Engl. 35 (1996) 1021.
[14] Y. Dai, R.M. Whittal, L. Li, Anal. Chem. 68 (1996) 2494.
[15] R. Kruger, A. Pfenninger, I. Fournier, M. Gluckmann, M. Karas, Anal. Chem. 73 (2001) 5812.
[16] V. Horneffer, R. Reichelt, K. Strupat, Int. J. Mass Spectrom. 226 (2003) 117.
[17] A.I. Gusev, O.J. Vasseur, A. Proctor, A.G. Sharkey, D.M. Hercules, Anal. Chem. 67 (1995) 4565.
[18] D. Figeys, Anal. Chem. 75 (2003) 2891.
[19] R.M. Caprioli, T.B. Farmer, J. Gile, Anal. Chem. 69 (1997) 4751.
[20] M. Stoeckli, T.B. Farmer, R.M. Caprioli, J. Am. Soc. Mass Spectrom. 10 (1999) 67.
[21] R.W. Garden, J.V. Sweedler, Anal. Chem. 72 (2000) 30.
[22] G. Piyadasa, J.R. McNabb, V. Spicer, K.G. Standing, W. Ens, Proceedings of the 52nd ASMS Conference on Mass Spectrometry and Allied Topics, Nashville, TN, 2004.
[23] H. Qiao, G. Piyadasa, O. Krokhin, V. Spicer, K.G. Standing, W. Ens, Proceedings of the 54th Conference on Mass Spectrometry and Allied Topics, Seattle, WA, 2006.
[24] W. Bouschen, B. Spengler, Int. J. Mass Spectrom. 266 (2007) 129.
[25] V.I. Kozlovski, A.V. Loboda, V. Spicer, J. McNabb, W. Ens, K.G. Standing, Proceedings of the 50th ASMS Conference on Mass Spectrometry and Allied Topics, Orlando, FL, USA, 2002.
[26] H. Qiao, V. Spicer, W. Ens, Rapid Commun. Mass Spectrom. 22 (2008) 2779.
[27] H.B. Bull, K. Breese, Arch. Biochem. Biophys. 161 (1974) 665.
[28] J. Kyte, R.F. Doolittle, J. Mol. Biol. 157 (1982) 105.

[29] (a) K.J. Stone, J.L. Strominger, Proc. Nat. Acad. Sci. U.S.A. 68 (1971) 3223; (b) National Center for Biotechnology Information (NCBI) database, accessed October 2008 at http://www.ncbi.nlm.nih.gov/.
[30] J. Kampmeier, K. Dreisewerd, M. Schurenberg, K. Strupat, Int. J. Mass Spectrom. Ion Process. 169/170 (1997) 31.
[31] J. Yao, J.R. Scott, M.K. Young, C.L. Wilkins, J. Am. Soc. Mass Spectrom. 9 (1998) 805.
[32] I. Fournier, R.C. Beavis, J.C. Blais, J.C. Tabet, G. Bolbach, Int. J. Mass Spectrom. Ion Process. 169/170 (1997) 19.
[33] I. Fournier, C. Marinach, J.C. Tabet, G. Bolbach, J. Am. Soc. Mass Spectrom. 14 (2003) 893.
[34] G. Matthias, M. Karas, J. Mass Spectrom. 34 (1999) 467.